JACS
JOURNAL OF THE AMERICAN CHEMICAL SOCIETY

Communication

pubs.acs.org/JACS

Simultaneous Noncovalent Modification and Exfoliation of 2D Carbon Nitride for Enhanced Electrochemiluminescent Biosensing

Jingjing Ji,[†] Jing Wen,[‡] Yanfei Shen,[†] Yanqin Lv,[†] Yile Chen,[†] Songqin Liu,[†] Haibo Ma,[‡] and Yuanjian Zhang*[,†]

[†]Jiangsu Engineering Laboratory of Smart Carbon-Rich Materials and Device, Jiangsu Province Hi-Tech Key Laboratory for Bio-Medical Research, School of Chemistry and Chemical Engineering, Medical School, Southeast University, Nanjing 211189, China

[‡]School of Chemistry and Chemical Engineering, Nanjing University, Nanjing 210023, China

Supporting Information

ABSTRACT: As an emerging nitrogen-rich 2D carbon material, graphitic carbon nitride (CN) has drawn much attention for applications ranging from photo-/electrocatalysts to biosensors. Interfacial modification of CN is fundamentally vital but is still in its infancy and remains challenging due to the low reactivity of CN. Here we report that, in conjunction with a π-π stacking interaction, bulk CN could be simultaneously exfoliated via facile mechanical grinding. The obtained CN nanosheets (m-CNNS) not only retained the pristine optoelectronic properties of bulk CN but also enriched a friendly interface for further coupling biomolecules with advanced properties, overcoming the deficiencies of CN in surface science. The m-CNNS were further covalently linked to a DNA probe, and the resultant electrochemiluminescent biosensor for the target DNA exhibited much enhanced sensitivity with respect to that obtained by direct physical absorption of the DNA probe on unmodified CNNS. This noncovalent exfoliation and interfacial modification should greatly expand the scope of potential applications of CN in areas such as biosensing and should also be applicable to other 2D materials in interface modulation.

As an important type of nanomaterials, 2D materials in which electrons are free to move but restricted in the third direction are highly desirable to obtain superior catalytic, photovoltaic, and electrochemical properties.[1] Graphitic carbon nitride (CN) has been recently discovered to be promising in applications ranging from photo-/electrocatalysis to smart assemblies, owing to its proper electronic structure, high stability, and wide availability.[2] Compared to other 2D materials, e.g., graphene, MoS_2, and black phosphorus, one of the attractive merits of CN is its organic nature; its molecular structure and electronic properties can be facilely modulated, e.g., by condensation of various monomers. For example, C_2N, C_3N_2, and C_3N_5 were reported recently with striking new properties,[3] beyond the common C_3N_4. Several pioneering works in preparing CN nanosheets (CNNS), typically by liquid exfoliation or thermal oxidation,[2i,j] have been reported, further boosting the activities and expanding the scope of potential applications of CN. Applications of CN have already been extended to bioimaging and luminescent immunoassay.[2i,4]

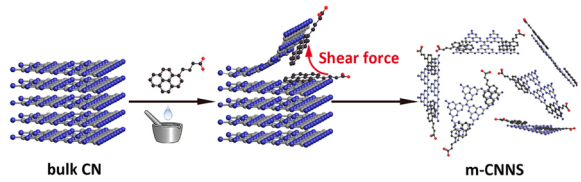

Figure 1. General exfoliation and modification process of carbon nitride (CN) via noncovalent π-π stacking interaction.

Several critical problems need to be addressed before the potential applications of the intriguing CN can be realized. First, the poor dispersion of CN in most solvents[2f] makes their processing difficult, similar to other nanocarbons such as carbon nanotubes and graphene.[2h,5] Moreover, the efficiency of exfoliating CNNS is still low; e.g., for a typical liquid exfoliation, a long sonication time up to ~16 h is needed to obtain CNNS with a low concentration of ~0.15 mg/mL.[2i] Last, pristine CNNS are chemically inert, making a reliable and robust linkage between CNNS and foreign molecules by normal methods difficult,[5c] which limits their practical biological applications.

Although recent advances in noncovalent functionalization of CN analogues such as carbon nanotubes and graphene may provide opportunities for addressing the above grand challenges,[5c−e] the exploration of noncovalent exfoliation and interfacial modification of CN has not yet been reported. Here we show that mechanical grinding of bulk CN with aromatic molecules could circumvent all the aforementioned difficulties by simultaneous exfoliation and modification of CN via π-π stacking interactions (Figure 1). In contrast to chemical tailoring such as hydrolysis in strong acids,[6] the structure and electronic properties of CN were not altered after the noncovalent modification when the new moiety was added on the surface, which not only improved dispersibility but also offered a friendly linker for foreign molecules with advanced properties. For example, 1-pyrenebutyrate (Py-COOH, sodium salt), containing a principal planar aromatic skeleton, was noncovalently modified on CN, which was further anchored with a DNA probe to fabricate a boosted electrochemiluminescent DNA biosensor. This type of noncovalent strategy has been overlooked as a way to prepare 2D

Received: June 28, 2017
Published: August 8, 2017

DOI: 10.1021/jacs.7b06708
J. Am. Chem. Soc. 2017, 139, 11698−11701

materials and may be applicable even if the modifier is not needed, since these organic "impurities" can be readily removed.

Figure 1 and the supplemental movie show the general exfoliation and modification processes for bulk CN. Briefly, Py-COOH (sodium salt) was dissolved in water, and then bulk CN powder was added. After that, a continuous shear force was applied to the mixture via manual mortar-and-pestle grinding or ball-milling for 2−4 h. After removal of large precipitates, a highly stable (zeta potential = −35.4 mV) and milky dispersion containing Py-COOH (sodium salt)-modified CNNS (namely m-CNNS) was obtained. In contrast, bulk CN alone cannot form a stable dispersion, even under the same grinding (Figure 2a,b

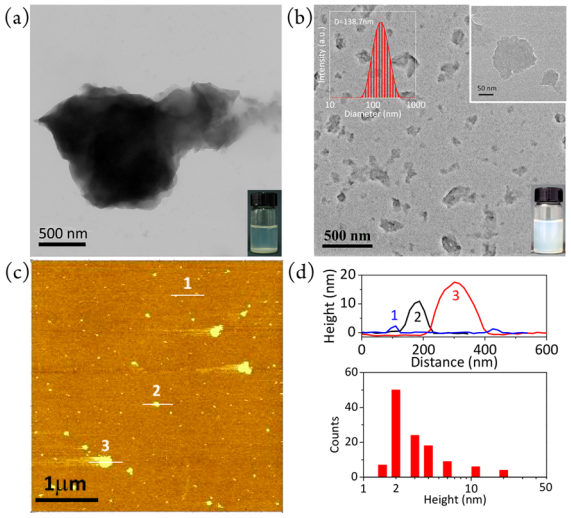

Figure 2. TEM images of (a) pristine bulk CN and (b) m-CNNS. Inset in (a) shows a photo of bulk CN dispersion with some suspended solid, and insets in (b) show a photo and the DLS size distribution of the m-CNNS dispersion. (c) AFM image of m-CNNS. (d) Height profiles of the points marked in (c) and height statistics of m-CNNS (N = 118) using the AFM data in (c).

insets, and Figure S1). Upon grinding, the van der Waals forces among CN layers would be temporarily weakened but recovered soon without application of continuous shear force; Py-COOH (sodium salt) could absorb onto the newly generated surface of CN during the continuous grinding and facilitate the exfoliation. Thus, few-layered CN could be stabilized against restacking due to the carboxyl groups that, as part of Py-COOH (sodium salt), induce repulsive forces among them (see Figure S1 and more discussion in the Supporting Information (SI)).

Successful exfoliation of pristine bulk CN to a few layers was verified by transmission/scanning electron microscopy (TEM/SEM) and atomic force microscopy (AFM). TEM/SEM images showed that the bulk CN mostly consisted of thick particles (Figures 2a and S2a), while m-CNNS was sheet-like, and the near transparency indicated its ultrathin thickness (Figures 2b and S2b). The AFM image (Figure 2c) and height profiles (Figure 2d) further demonstrated the thickness of m-CNNS ranging from 1.5 to 20 nm, with a typical value of ∼2 nm. Moreover, after grinding exfoliation, as observed from both TEM and dynamic light scattering (DLS) measurement, the lateral size of m-CNNS (∼138.7 ± 0.7 nm) became smaller in comparison with the pristine bulk CN particles (∼ several micrometers) but was still a bit larger than that traditional liquid-exfoliated CNNS (∼111.4 ± 1.5 nm, Figure S3).[2i] To complement these results, X-ray diffraction (XRD) of bulk CN before and after grinding with Py-COOH (sodium salt) was studied. In general, the XRD pattern of the bulk CN has two characteristic diffraction peaks (Figure 3a), one at 13.1° showing the in-plane ordering (100) of the

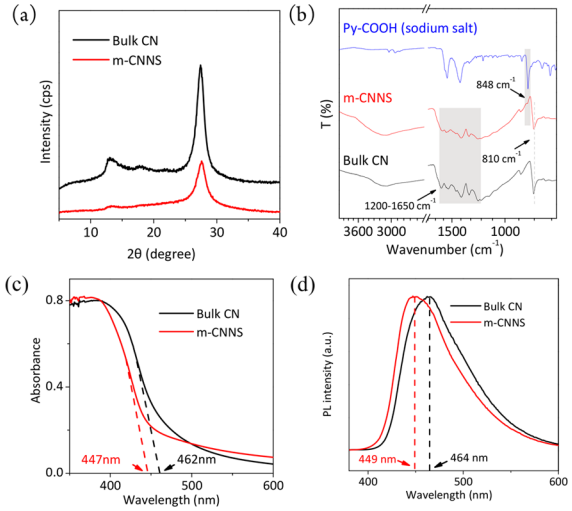

Figure 3. (a) XRD pattern and (b) FT-IR spectra of m-CNNS, bulk CN, and Py-COOH (sodium salt). (c) UV/vis and (d) PL spectra of bulk CN and m-CNNS powders.

graphitic motif and the other, stronger one at 27.4° assigned to the graphitic interlayer (002) structure. Noticeably, these two peaks were both greatly reduced in m-CNNS, showing a less periodic texture—important evidence of the successful exfoliation of bulk CN into a few layers.[2j] Moreover, compared to those of bulk CN, the N_2 isothermal absorption/desorption curves of lyophilized m-CNNS powder (Figure S4) exhibited new slit-shaped pores and an evident boosted BET surface area up to 7 times that of bulk CN, a typical characteristic of exfoliation of nanosheets.

To get insight into possible changes in chemical structures, the Fourier transform infrared (FT-IR) spectrum of m-CNNS was studied (Figure 3b), which was reminiscent of that of bulk CN, both having a strong peak at ∼810 cm^{-1} (tri-*s*-triazine ring sextant out-of-plane bending) and stretching vibration modes at 1200−1650 cm^{-1} (CN heterocycles). This result suggested that the primary framework of tri-*s*-triazine structure was not altered after grinding. Nevertheless, compared with that of bulk CN, the FT-IR spectrum of m-CNNS showed an additional minor peak at 848 cm^{-1}, originating from the C−H wagging vibration of Py-COOH (sodium salt).[7] Thus, thanks to the π-π interaction, the typical CN molecular structure was not altered in m-CNNS (see Figure S5 and more discussion in SI).

The optical properties of m-CNNS were investigated by UV/vis absorption and photoluminescence (PL) spectra. The characteristic semiconductor absorption edge of m-CNNS (Figure 3c) was mostly retained with only a slight blue shift of 15 nm compared to bulk CN. Similarly, the PL of m-CNNS also exhibited a minor blue shift (Figure 3d). Because the PL of Py-COOH (sodium salt) occurred at a higher wavelength (Figure S6), the slight blue-shifts in the spectra of m-CNNS with respect to those of bulk CN should be mainly ascribed to the decreased size of CN, a quantum confinement effect.[6a] Nevertheless, compared to that of strong acids-tailored bulk CN that had many newly generated oxygen-containing defects, herein the PL blue-shift of m-CNNS was small and negligible.[6] Thus, the noncovalent exfoliation and modification using Py-COOH

DOI: 10.1021/jacs.7b06708
J. Am. Chem. Soc. 2017, 139, 11698−11701

(sodium salt) did not interrupt the extended π-system of bulk CN, and the original optical properties of pristine CN were well maintained (see Figure S6 and more discussion in the SI), which is vital to many potential applications. Except for negative-charged Py-COOH (sodium salt), 1-pyrene-methanamine (Py-NH_2), a positive-charged pyrene derivative, was also used to exfoliate CN as a control, but a stable dispersion could not be easily obtained due to the electrostatic interaction-induced aggregation of opposite-charged Py-NH_2 and CN (Figure S7). It is supposed that the surface charge of aromatic molecules is also vital for the successful noncovalent exfoliation and dispersion of CNNS.

To get further insights into the molecular assembly of the Py-COOH (sodium salt) that shows outstanding performance in exfoliating bulk CN, we carried out density functional theory (DFT) calculations to analyze the adsorption models and adsorption abilities of H_2O and pyrene (the side chain is omitted) on the surface of CNNS (see computational methods in SI). As shown in Figure 4a,b, the interfacial adsorption[8] was

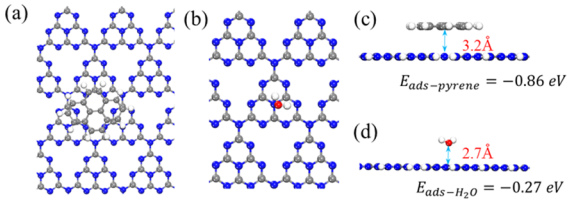

Figure 4. Theoretical calculations of adsorption models. (a,b) Optimized adsorption structures of pyrene/CNNS and H_2O/CNNS. (c,d) Corresponding adsorption energies and relative positions.

the main focus in our calculations, because interlayer adsorption is usually considered as the driving force for liquid exfoliation. The adsorption energies per H_2O and pyrene molecules on CNNS were calculated to be −0.27 and −0.86 eV, respectively. This indicates that pyrene has a stronger absorption ability than a H_2O molecule toward CNNS and can serve as an efficient substance to exfoliate bulk CN. The high stability of the pyrene/CN complex could be also verified by the recent computations of the hybrid complex of acene-type planar carbon-dot (C-dot) and CN.[9] Our calculations of the absorption energy and position (on top of the C and N atoms) for the H_2O molecule were also in agreement with recent gas-phase calculations.[8a] In addition, as shown in Figure 4c,d, the adsorption distance between pyrene and CN was calculated to be ~3.2 Å, in the typical range for π-π interactions. For the H_2O molecule absorbed on the surface of CNNS, the distance from the O atom to CNNS was 2.7 Å, and the dihedral angle between H_2O and CNNS was ~35°, both suggesting a weak physical adsorption. In this context, by theoretical calculation, pyrene was thermodynamically preferred to be absorbed on the surface of CN to exfoliate bulk CN into CNNS rather than water molecules, which were previously reported to exfoliate bulk CN by long-time sonication,[2i] and this was well consistent with the experimental results.

Thus, by simple one-step grinding, bulk CN could be facilely exfoliated into few-layered CNNS via π-π interactions between bulk CN and Py-COOH (sodium salt). This strategy was also applicable to other aromatic molecules such as congo red (CR, Figure S8). Compared with sonication, which is also widely used in exfoliating layered materials, the grinding method was time-saving and had an evidently higher capacity for loading of functional conjugated molecules (see experimental details in the SI). As a result, the interface of CN was significantly modified, which not only made CN well dispersed in aqueous solution but also would facilitate the further coupling of molecules in a robust and reliable manner without disrupting the electronic structure of CN.

Electrochemiluminescence (ECL) is an emission process whereby excited states are generated by electrochemical reactions in the presence of co-reactants.[10] Due to the absence of a photoexcitation background, ECL biosensors have attractive features such as high sensitivity over the PL technique.[10b] Many ECL luminophors have been developed, such as Ru complex, luminol, and quantum dots. As an emerging luminophor, CNNS has attracted attention very recently due to its merits including good biocompatibility, controllable band gap luminescence and low cost, compared to its counterparts.[4b] On the other hand, high-performance biosensors often necessitate effective immobilization of biomolecules at sensor interfaces. Nevertheless, traditional CNNS prepared by sonication-assisted liquid-phase exfoliation had few active moieties; thus, it could not meet the criteria for robust coupling of biomolecules. Thus, to verify if the as-obtained m-CNNS had a friendly interface for efficiently anchoring biomolecules, a well-developed DNA probe was selected as a model biomolecule to conjugate on the m-CNNS surface by using Py-COOH (sodium salt) as the covalent linker. As shown in Figure 5a, an amino-terminated probe ssDNA

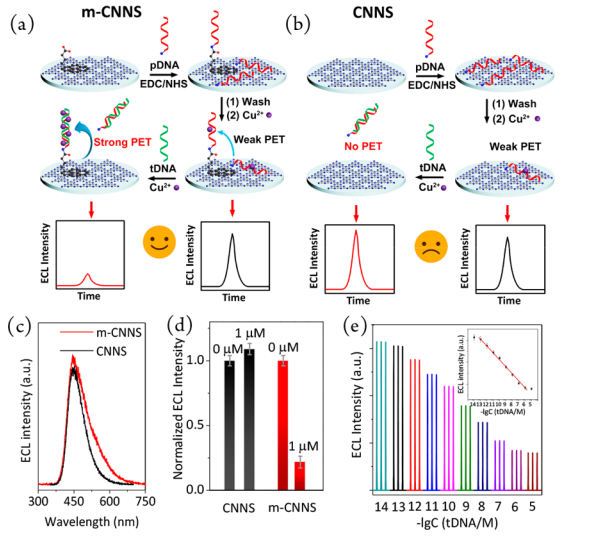

Figure 5. Preparation of ECL biosensor on glassy carbon electrode using m-CNNS (a) and conventional CNNS (b). ECL emission spectra of m-CNNS and CNNS (c). ECL intensity of m-CNNS- and CNNS-based biosensor upon addition of 0 and 1 μM tDNA (d). ECL response of m-CNNS upon addition of 10^{-14}–10^{-5} M tDNA (e). Inset: scatter plot and linear fitting of ECL intensity vs concentration.

(pDNA) was conjugated to the carboxylic groups of Py-COOH (sodium salt) facilely using EDC/NHS activation, a general cross-linking method that is also applicable to connect m-CNNS with other biomolecules such as antibody, aptamer, and enzyme. Based on the complementary base-pairing principle, the target ssDNA (tDNA) can be captured, forming a tDNA-pDNA hybrid. Taking m-CNNS as the luminophor, an ECL biosensor for tDNA was constructed. As a control, a similar ECL sensor using traditional CNNS was also constructed (Figure 5b).

ECL spectra in Figure 5c show that m-CNNS had a similar emission wavelength compared to traditional CNNS, indicating that the interfacial modification of Py-COOH (sodium salt) did

DOI: 10.1021/jacs.7b06708
J. Am. Chem. Soc. 2017, 139, 11698–11701

not alter the ECL property, an appealing aspect of noncovalent modification.[5c−e] In addition, the ECL signal of m-CNNS was stable under continuous cyclic voltammetric scans on glassy carbon electrode (Figure S9), a prerequisite for ECL biosensors. Since Cu^{2+} can bind to the N7 position of DNA bases, forming a DNA-Cu^{2+} complex,[11] the amount of Cu^{2+} absorbed on DNA was proportional to the total amount of DNA. Further considering the fact that the ECL emission of CNNS could be quenched by Cu^{2+}, the decrease of ECL intensity would be proportional to the increase of the amount of DNA on the electrode surface. Thus, when tDNA was captured, more absorbed Cu^{2+} would lead to a stronger quenching of the ECL of CNNS. For example, upon addition of 1 μM tDNA, a pronounced decrease of ECL intensity (78.23%) was observed (Figure 5d). Such inverse relationship between the amount of tDNA and ECL intensity could be further utilized to quantify the concentration of tDNA. Figure 5e shows that the ECL intensity decreased with increasing concentration of tDNA, exhibiting a fine linear correlation in a broad range from 10^{-6} to 10^{-13} M, with a very low detection limit of 3.6×10^{-14} M (S/N = 3). The excellent performance of the proposed sensor already makes it one of the most sensitive signal-amplification-free biosensors for DNA (Table S1). As a control, instead of covalent linkage, pDNA was immobilized on conventional CNNS by direct physical absorption (Figure 5b).[4a] However, only a minor increase in ECL intensity (9%), equivalent to system error, was observed upon the addition of tDNA under the same conditions (see further discussion in SI). This suggests that the more sufficient and reliable linkage between pDNA and m-CNNS greatly promoted the ECL sensitivity. Such enhancements were largely dependent on the improvement of CN interfacial properties by using Py-COOH (sodium salt) as the modifier.

In summary, we have developed a noncovalent way to simultaneously modify and exfoliate bulk CN with aromatic molecules via facile mechanical grinding. It not only mostly retained the pristine optoelectronic properties of bulk CN but also modified the interface properties of the as-exfoliated CNNS. The as-obtained CNNS could be well dispersed in aqueous solution and, more strikingly, had a friendly interface for further efficient conjugation of biomolecules, addressing the challenges in potential biosensing applications of CN. For example, using the modified CNNS, an ECL biosensor with a covalently linked DNA probe was proposed that exhibited much enhanced sensitivity compared to conventional CNNS with direct physical absorption. This work opens a new avenue to exfoliate CN and couple functional molecules on CN that is not only applicable to biomolecules but also extendable to many other systems with desired properties, such as smart molecules and nanoparticles.[5f]

■ ASSOCIATED CONTENT

Supporting Information

The Supporting Information is available free of charge on the ACS Publications website at DOI: 10.1021/jacs.7b06708.

Experimental and calculation details; BET, XPS, and SEM images; table comparing the performance of the m-CNNS-based ECL sensors; and more control results, including Figures S1−S9 (PDF)

Supplemental movie showing preparation of m-CNNS by manual mortar-and-pestle grinding (AVI)

■ AUTHOR INFORMATION

Corresponding Author

*yuanjian.zhang@seu.edu.cn

ORCID

Songqin Liu: 0000-0002-4686-5291

Haibo Ma: 0000-0001-7915-3429

Yuanjian Zhang: 0000-0003-2932-4159

Notes

The authors declare no competing financial interest.

■ ACKNOWLEDGMENTS

This work was supported by the National Natural Science Foundation of China (21675022, 21627806), the Natural Science Foundation of Jiangsu Province (BK20160028, BK2017-0084), the Open Funds of the State Key Laboratory of Electroanalytical Chemistry (SKLEAC201703), and the Fundamental Research Funds for the Central Universities.

■ REFERENCES

(1) Tan, C.; et al. *Chem. Rev.* **2017**, *117*, 6225.

(2) (a) Wang, X.; Maeda, K.; Thomas, A.; Takanabe, K.; Xin, G.; Carlsson, J. M.; Domen, K.; Antonietti, M. *Nat. Mater.* **2009**, *8*, 76. (b) Xu, J.; Brenner, T. J. K.; Chabanne, L.; Neher, D.; Antonietti, M.; Shalom, M. *J. Am. Chem. Soc.* **2014**, *136*, 13486. (c) Liu, J.; et al. *Science* **2015**, *347*, 970. (d) Pei, Z.; Gu, J.; Wang, Y.; Tang, Z.; Liu, Z.; Huang, Y.; Huang, Y.; Zhao, J.; Chen, Z.; Zhi, C. *ACS Nano* **2017**, *11*, 6004. (e) Ma, T. Y.; Dai, S.; Jaroniec, M.; Qiao, S. Z. *Angew. Chem., Int. Ed.* **2014**, *53*, 7281. (f) Zhou, Z.; Wang, J.; Yu, J.; Shen, Y.; Li, Y.; Liu, A.; Liu, S.; Zhang, Y. *J. Am. Chem. Soc.* **2015**, *137*, 2179. (g) Zhang, Y.; Zhou, Z.; Shen, Y.; Zhou, Q.; Wang, J.; Liu, A.; Liu, S.; Zhang, Y. *ACS Nano* **2016**, *10*, 9036. (h) Gai, P.; Song, R.; Zhu, C.; Ji, Y.; Chen, Y.; Zhang, J.-R.; Zhu, J.-J. *Chem. Commun.* **2015**, *51*, 14735. (i) Zhang, X.; Xie, X.; Wang, H.; Zhang, J.; Pan, B.; Xie, Y. *J. Am. Chem. Soc.* **2013**, *135*, 18. (j) Niu, P.; Zhang, L.; Liu, G.; Cheng, H. M. *Adv. Funct. Mater.* **2012**, *22*, 4763.

(3) (a) Fechler, N.; Zussblatt, N. P.; Rothe, R.; Schlögl, R.; Willinger, M.-G.; Chmelka, B. F.; Antonietti, M. *Adv. Mater.* **2016**, *28*, 1287. (b) Mahmood, J.; et al. *Proc. Natl. Acad. Sci. U. S. A.* **2016**, *113*, 7414. (c) Yang, S.; et al. *Adv. Mater.* **2017**, *29*, 1605625. (d) Mane, G. P.; Talapaneni, S. N.; Lakhi, K. S.; Ilbeygi, H.; Ravon, U.; Al-Bahily, K.; Mori, T.; Park, D.-H.; Vinu, A. *Angew. Chem., Int. Ed.* **2017**, *56*, 8481.

(4) (a) Wang, Q.; Wang, W.; Lei, J.; Xu, N.; Gao, F.; Ju, H. *Anal. Chem.* **2013**, *85*, 12182. (b) Zhou, Z.; Shang, Q.; Shen, Y.; Zhang, L.; Zhang, Y.; Lv, Y.; Li, Y.; Liu, S.; Zhang, Y. *Anal. Chem.* **2016**, *88*, 6004.

(5) (a) Hirsch, A. *Angew. Chem., Int. Ed.* **2002**, *41*, 1853. (b) Tung, V. C.; Allen, M. J.; Yang, Y.; Kaner, R. B. *Nat. Nanotechnol.* **2009**, *4*, 25. (c) Chen, R. J.; Zhang, Y.; Wang, D.; Dai, H. *J. Am. Chem. Soc.* **2001**, *123*, 3838. (d) Ehli, C.; Oelsner, C.; Guldi, D. M.; Mateo-Alonso, A.; Prato, M.; Schmidt, C.; Backes, C.; Hauke, F.; Hirsch, A. *Nat. Chem.* **2009**, *1*, 243. (e) Georgakilas, V.; Tiwari, J. N.; Kemp, K. C.; Perman, J. A.; Bourlinos, A. B.; Kim, K. S.; Zboril, R. *Chem. Rev.* **2016**, *116*, 5464. (f) Srinivasan, S.; Shin, W. H.; Choi, J. W.; Coskun, A. *J. Mater. Chem. A* **2013**, *1*, 43.

(6) (a) Zhou, Z.; Shen, Y.; Li, Y.; Liu, A.; Liu, S.; Zhang, Y. *ACS Nano* **2015**, *9*, 12480. (b) Zhang, J.; Zhang, M.; Lin, L.; Wang, X. *Angew. Chem., Int. Ed.* **2015**, *54*, 6297.

(7) Liu, Y.; et al. *Nat. Commun.* **2014**, *5*, 5461.

(8) (a) Wu, H. Z.; Liu, L. M.; Zhao, S. J. *Phys. Chem. Chem. Phys.* **2014**, *16*, 3299. (b) Aspera, S. M.; David, M.; Kasai, H. *Jpn. J. Appl. Phys.* **2010**, *49*, 115703.

(9) Gao, G.; Jiao, Y.; Ma, F.; Jiao, Y.; Waclawik, E.; Du, A. *Phys. Chem. Chem. Phys.* **2015**, *17*, 31140.

(10) (a) Faulkner, L. R.; Bard, A. J. *J. Am. Chem. Soc.* **1968**, *90*, 6284. (b) Wu, P.; Hou, X.; Xu, J.-J.; Chen, H.-Y. *Chem. Rev.* **2014**, *114*, 11027.

(11) Gao, Y. G.; Sriram, M.; Wang, A. H. *Nucleic Acids Res.* **1993**, *21*, 4093.

DOI: 10.1021/jacs.7b06708
J. Am. Chem. Soc. 2017, 139, 11698−11701